Two-Mode Entanglement in Spin and Spatial Degrees of Freedom

Dipl.-Phys. **Karsten Lange**,
geboren am 16. Juli 1987 in Salzweldel

2018

Referent: Apl. Prof. Dr. Carsten Klempt,
Institut für Quantenoptik, Hannover

Korreferent: Prof. Dr. Silke Ospelkaus,
Institut für Quantenoptik, Hannover

Korreferent: Prof. Dr. Géza Tóth,
Department of Theoretical Physics, Bilbao

Abstract

The predictions of quantum mechanics often differ from our everyday experiences. In the classical case, the state of a system can be predicted precisely, assuming the exact knowledge of all parameters. This is not possible in quantum mechanics. For example, the spin of one particle can be simultaneously in two different states, until a measurement defines the actual state. If multiple particles are in such superposition states, their spins can be coupled with each other such that the measurement of one particle changes the physical state of the other particles. This coupling effect is a fundamental part of quantum mechanics and is called entanglement. It is a central requirement for applications in the fields of quantum communication, quantum cryptography and quantum computing. One possibility to create entanglement are spin-changing collisions in a spinor Bose-Einstein condensate. These collisions are described by a nonlinear process, which creates non-classical correlations between all atoms of the Bose-Einstein condensate.

Within this thesis, ^{87}Rb spinor Bose-Einstein condensates are used to demonstrate Einstein-Podolsky-Rosen entanglement by the generation and analysis of a two-mode entangled state in spin space [A1]. These states are applied in an interferometric measurement with a resolution of $2.05^{+0.34}_{-0.37}$ dB beyond the standard quantum limit [A2]. Depending on the dynamics, the process can also be analogous to the dynamical Casimir effect [A3]. The entanglement between the particles in these publications is strongly connected with their indistinguishability. It is thus possible to make the particles distinguishable again and recover the entanglement between the now separated particles? This question is approached by cutting an entangled state of indistinguishable particles into two spatially separated atomic modes - creating a two-mode entangled state in real space. As shown in Ref. [A4], the entanglement between the two separated clouds of a Bose-Einstein condensate can be measured directly. In the future, the created state can be employed for a test of quantum nonlocality.

Zusammenfassung

Die Vorhersagen der Quantenmechanik stehen oft im Widerspruch mit unseren alltäglichen Erfahrungen. Im klassischen Fall kann der Zustand eines Systems bei genauer Kenntnis aller Parameter präzise vorausgesagt werden. Quantenmechanisch ist dies nicht möglich. Der Spin eines Teilchens kann sich beispielsweise gleichzeitig in zwei verschiedenen Zuständen befinden, bis eine Messung seinen Zustand definiert. Befinden sich mehrere Teilchen in Superpositionszuständen, können ihre Spins miteinander gekoppelt sein, sodass die Messung eines Teilchens den physikalischen Zustand der anderen Teilchen ändert. Dieser Kopplungseffekt ist fundamentaler Bestandteil der Quantenmechanik und wird Verschränkung genannt. Er ist eine zentrale Voraussetzung für viele Anwendungen in den Forschungsfeldern Quantenkommunikation, Quantenkryptographie und Quanteninformationsverarbeitung. Eine Möglichkeit Verschränkung zu erzeugen sind Spin-ändernde Stöße in einem Spinor-Bose-Einstein-Kondensat. Diese Stöße werden durch einen nichtlinearen Prozess beschrieben, der nichtklassische Korrelationen zwischen allen Atomen des Bose-Einstein-Kondensats erzeugt. Innerhalb dieses Arbeit werden ^{87}Rb Spinor-Bose-Einstein-Kondensate genutzt um Einstein-Podolsky-Rosen-Verschränkung durch die Analyse eines zwei-moden verschränkten Zustandes nachzuweisen [A1]. Diese Zustände werden in einer interferometrischen Messung genutzt, um eine Auflösung von $2.05^{+0.34}_{-0.37}$ dB jenseits des Standard-Quantum-Limits zu erreichen. Abhängig von der Art der Anregung ist der Prozess analog zum dynamischen Casimir-Effekt [A3]. Die Verschränkung der Teilchen ist in diesen Arbeiten stark mit ihrer Ununterscheidbarkeit verknüpft. Ist es möglich die Teilchen wieder unterscheidbar zu machen und die Verschränkung zwischen den nun separierten Teilchen zu erhalten? Um diese Frage zu beantworten wird ein verschränkter Zustand ununterscheibarer Teilchen in zwei räumlich getrennte Moden geteilt - was einen zwei-moden verschränkten Zustand im realen Raum erzeugt. In Ref. [A4] wird gezeigt, dass die Verschränkung zwischen zwei getrennten atomaren Wolken eines Bose-Einstein-Kondensats direkt gemessen werden kann. In der Zukunft kann der Zustand für einen Test der Nichtlokalität verwendet werden.

Schlagwörter: Bose-Einstein-Kondensat, Spindynamik, Verschränkung

Contents

1 Introduction

God does not play dice with our universe.

A. Einstein

This statement expresses Einstein's opinion that no theory with intrinsic uncertainties can be complete. He assumes that, they only appear due to a lack of information about the system. Consequently, no real uncertainties exist from Einstein's point of view. This statement is correct in the classical description of our world. However, it is not valid on scales at which the wave nature of matter is important. The transition between these two regions is subject of state-of-the-art research [1, 2, 3]. Measurement devices, in particular atom interferometers, operating in the quantum regime have a broad range of applications. They are used to measure gravitational acceleration [4, 5], the rotation of the earth [6, 7, 8], the time [9, 10] and physical constants for example the gravitational [11, 12] or the fine-structure constant [13, 14]. Furthermore, atom clocks operate with an outstanding stability [10]. Despite the rapid technical progress, the accuracy of these measurements is fundamentally limited by shot noise or projection noise. This noise occurs from counting uncorrelated particles and gives rise to the standard quantum limit, which scales as $1/\sqrt{N}$ with the number of particles N. By inducing non-classical correlations between the particles, the standard quantum limit can be overcome and thus enhance the measurement precision [15]. These strong and non-classical correlations are called entanglement and are a pure quantum mechanical property. Using entangled states to enhance the measurement precision is realized with thermal atoms [16] and as presented in this thesis with Bose-Einstein condensates. For certain entangled states, the measurement precision is only limited by the fundamental Heisenberg limit, which scales as $1/N$. Entangled states are a crucial resource in the research fields of quantum communication [17], quantum cryptography [18], quantum sensors [19] and quantum information processing [20]. Up to know fully controllable entangled states of ten photons [21] and 20 ions [22] have been created, while in Bose-Einstein condensates states with 910 entangled atoms [23] have been generated at the cost of the individual control of the particles.

This thesis compares different possibilities to generate entanglement and shows how indistinguishability and entanglement are connected with each other in Bose-Einstein condensates. In the first chapter of this thesis, squeezing is explained on the example of a harmonic oscillator. The next chapter addresses the question how entanglement can be created and classified. Therefore, different methods to create entanglement in Bose-Einstein condensates with non-linear atom-atom interactions are compared. Using the results of this chapter, an overview about the commonly used measures of entanglement is given. The last chapter addresses the question how a Bell test can be realized with the state characterized in Ref. [A4].

2 Squeezing

The mathematical description of a quantized single-mode field is equivalent to a quantum harmonic oscillator [24]. Therefore, the harmonic oscillator is taken as example to introduce the concepts of quadrature squeezing and homodyne detection.

2.1 Single-mode quadrature squeezed states

The Hamiltonian of a single-mode harmonic oscillator is given by $H = \omega(a^\dagger a + 1/2)$ with the creation and annihilation operators $a^\dagger$ and a. These operators define to the quadratures $X = 1/\sqrt{2}(a+a^\dagger)$ and $P = \mathrm{i}/\sqrt{2}(a-a^\dagger)$. They oscillate $90°$ phase-shifted with the frequency ω and can be interpreted as dimensionless field amplitudes, e.g. as position and momentum of a classical harmonic oscillator or as amplitude of an electro-magnetic wave. The ground-state wave function of a harmonic oscillator is then given by $\Psi_0(X) = \pi^{-1/4}\,\mathrm{e}^{-X^2/2}$ or equivalently by $\tilde{\Psi}_0(P) = \pi^{-1/4}\,\mathrm{e}^{-P^2/2}$. Vacuum fluctuations lead to non-zero uncertainties in the quadratures of the ground state in contrast to the classical case. This quantum mechanical uncertainty is equally distributed among the quadratures $\Delta X = \Delta P = 1/2$ (see Fig. 2.1a). While the product of both quadrature uncertainties is bounded by the Heisenberg uncertainty principle $\Delta X \Delta P \geq 1/4$, it is possible to reduce one uncertainty at the cost of the other. These states are called single-mode squeezed states. In consequence this means, that the uncertainty of one quadrature can be smaller then $1/2$. The mathematical description follows Ref. [25]. By introducing the squeezing parameter $R > 0$, the squeezed wave functions can be written as $\Psi_R(X) = \sqrt{R}/(\pi^{1/4})\,\mathrm{e}^{-(XR)^2/2}$ and $\Psi_R(P) = 1/(\pi^{1/4}\sqrt{R})\,\mathrm{e}^{-(P/R)^2/2}$. The uncertainties of the quadratures are then given by $\langle \Delta X^2 \rangle = 1/(2R^2)$ and $\langle \Delta P^2 \rangle = R^2/2$. Reproducing the result of the unsqueezed state for $R = 1$ and for any other value of R leading to a single-mode squeezed state. These single-mode squeezed states can be decomposed into a superposition of even Fock states $\Psi_R = 1/\sqrt{\cosh R}\sum_{n=0}\sqrt{(2n)!}/2^n n!(-\tanh R)^2\,|2n\rangle$. This representation shows that squeezed states contain many excited states as shown in Fig. 2.1b.

2.2 Two-mode quadrature squeezed states

The system is now expanded to two coupled harmonic oscillators. The X quadratures of both oscillators (and also the P quadratures) therefore depend on each other. If the coordinates $X_\mathcal{A}$ and $P_\mathcal{A}$ are measured in different realizations, they can be used to predict $X_\mathcal{B}$ and $P_\mathcal{B}$ with an uncertainty depended on the coupling between the oscillators. If the correlations are strong enough this leads to two-mode squeezed states. A two-mode squeezed state in a cavity system is shown in Fig. 2.2. A simple example is the two-mode squeezed vacuum, whose wave functions can be written as $\Psi_R(X_\mathcal{A}, X_\mathcal{B}) = 1/\sqrt{\pi}\,\mathrm{e}^{-(X_\mathcal{A}+X_\mathcal{B})^2/(4R^2)}\,\mathrm{e}^{-R^2(X_\mathcal{A}-X_\mathcal{B})^2/4}$ and $\Psi_R(P_\mathcal{A}, P_\mathcal{B}) = 1/\sqrt{\pi}\,\mathrm{e}^{-(P_\mathcal{A}-P_\mathcal{B})^2/(4R^2)}\,\mathrm{e}^{-R^2(P_\mathcal{A}+P_\mathcal{B})^2/4}$. As indicated before, the correlations do not show in the individual X and P quadratures, instead they are in the sum of the P quadratures and the difference of the X quadratures. For $R > 1$, these correlations are squeezed and for R=0 the individual quadratures are independent. The Fock state basis
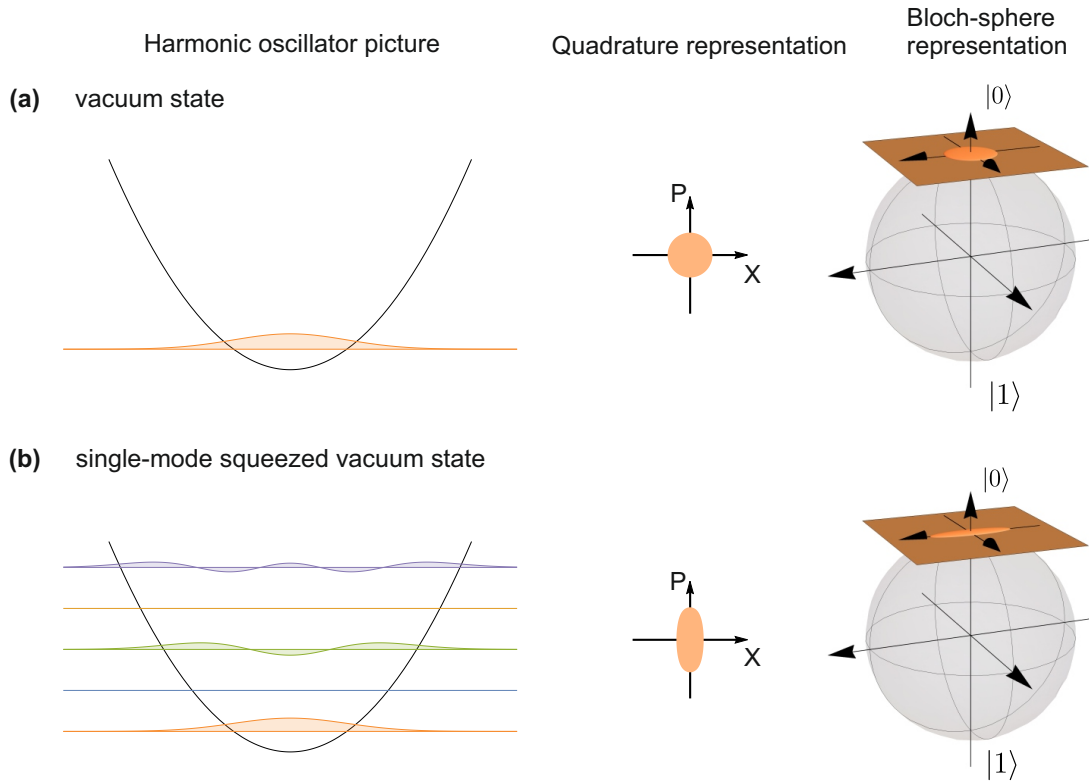
Figure 2.1: Different representations of **(a)** the vacuum state of the harmonic oscillator. The potential is shown as black line and the abscissa can correspond to either the X quadrature or P quadrature. The ground-state wave function corresponds to a disk in the quadrature picture. For a single-mode squeezed state **(b)** the wave function is a superposition of many weighted wave functions of even excited states. This effect Bose-Einstein condensateomes visible in the quadrature picture. Furthermore, the quadrature representation can be seen as an approximation in the Bloch-sphere picture, visualized as brown tangent plain at the north pole of the Bloch spheres. The south pole corresponds to the mode of local oscillator $|0\rangle$ and the north pole to the harmonic oscillator $|1\rangle$.

representation is given by $\Psi_R = {}^1\!/\!\cosh R \sum_{n=0}(\tanh R)^n |n, n\rangle$. In this description, the fact that only twin Fock states contribute to the state becomes obvious.

2.3 Homodyne Detection and the Bloch sphere

To access the quadratures experimentally, the mode has to be coupled with a strong classical field, the so-called local oscillator. The coupling leads to an enhancement of the signal by a factor $2\sqrt{N_{\mathrm{LO}}}$ with the local oscillator particle number N_{LO}. The local oscillator phase
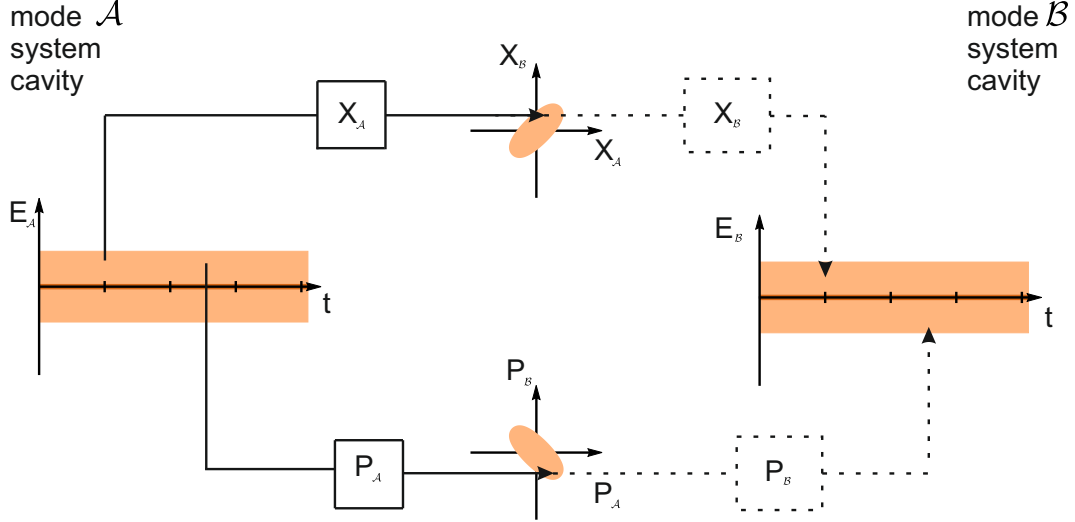
3

Figure 2.2: A two-mode squeezed state shown in the electro-magnetic wave and quadrature representation. While the uncertainties of each state are above the standard quantum limit (orange areas), the correlations between the X- and P-quadratures show squeezed fluctuations. Therefore, with a measurement of the electric field of $\mathcal{A}$ (full lines), it is possible to predict the same quadrature of state $\mathcal{B}$ (dashed lines) with an uncertainty below the standard quantum limit .

determines the direction of the phase-space displacement yielding the general quadrature $X_\theta = X\cos\theta + P\sin\theta$ with the quadrature angle θ [25]. This coupling is realized by a beam splitter operation between the modes of the harmonic and local oscillator. The population of each beam splitter port has to be measured. Furthermore, by tuning the phase of the local oscillator, homodyning can be seen as a tool to measure the density matrix of the underlying quantum state [26]. To describe and visualize the coupling process the multi-particle Bloch sphere is used. In our description, the north pole corresponds to the mode of the local oscillator $|0\rangle$ and the south pole to the quantum state $|1\rangle$, which we want to analyze. The main axes of the sphere are defined by the collective spin operators $J_x = 1/2(a^\dagger b + b^\dagger a)$, $J_y = 1/2\mathrm{i}(a^\dagger b - b^\dagger a)$ and $J_z = 1/2(a^\dagger a - b^\dagger b)$ with the bosonic annihilation a and b and creation operators $a^\dagger$ and $b^\dagger$ of the modes $|0\rangle$ and $|1\rangle$. They obey the commutation relations for angular momentum operators $[J_k, J_l] = \mathrm{i}\epsilon_{klm}J_m$, which results in the uncertainty relations $\Delta J_k \Delta J_l \geq 1/2|\langle J_m\rangle|$. The quadrature description can be seen as an approximation in the Bloch-sphere picture, visualized as a tangent plane at one pole of the Bloch sphere (see Fig. 2.1). In this framework the quadrature description is called parametric approximation and the quadratures can be obtained from the vector components according to $X = \sqrt{2/N}J_\mathrm{x}$ and $P = -\sqrt{2/N}J_\mathrm{y}$. The highly populated mode $|0\rangle$ belonging to the opposite pole is replaced conforming to $\langle a_0^\dagger a_0\rangle = N$.

3 Entanglement generation based on atomic interactions

The concepts developed for the harmonic oscillator are transferred to spinor Bose-Einstein condensates. The non-classical correlations arise in the spin and spatial degrees of freedom. This chapter compares different techniques to create entanglement. A common way to quantify the amount of squeezing compares the squeezed fluctuations to the standard quantum limit and gives the suppression in dB. The arrangement of the chapter follows the structure of Fig. 3.1.
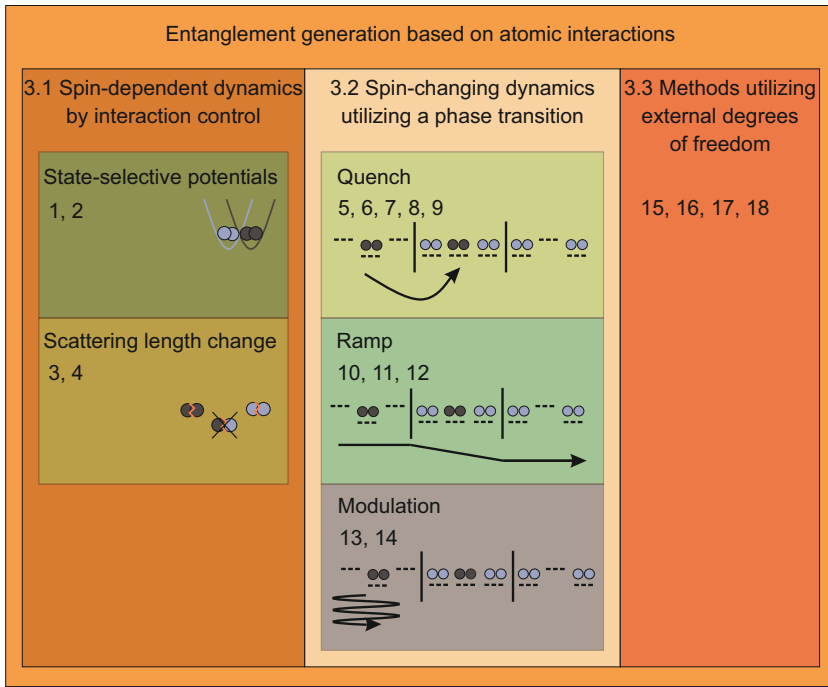
1	Riedel et al.	[27]
2	Fadel et al.	[28]
3	Strobel et al.	[29]
4	Muessel et al.	[30]
5	Kunkel et al.	[31]
6	Hamley et al.	[32]
7	Peise et al.	[A1]
8	Kruse et al.	[A2]
9	Lange et al.	[A4]
10	Luo et al.	[23]
11	Zou et al.	[33]
12	Hoang et al.	[34]
13	Hoang et al.	[35]
14	Lange et al.	[A3]
15	Bucker et al.	[36]
16	Hofferberth et al.	[37]
17	Lopes et al.	[38]
18	Estève et al.	[39]

Figure 3.1: Entanglement generation in spinor Bose-Einstein condensates by utilizing atomic interactions in ^{87}Rb. In the left column the atomic collisions between the atoms in the level $F = 1$, $m_F = -1$ and $F = 2$, $m_F = +1$ are tuned to create non-classical states. This can either be done with a state dependent potential or by utilizing a Feshbach resonance. In the middle group, the transitions between the polar, broken-axisymmetry and twin Fock phase can be exploited with a quench, ramp or modulation of the quadratic Zeeman energy to create entanglement. The insets visualize the ground state occupation probabilities in $F = 1$, $m_F = -1, 0, 1$ (from left to right). The right column shows all approaches, which utilize an external degree of freedom.

Linear coupling interactions between the modes just rotate spins on the Bloch sphere and hence do not create correlations between them [40]. Therefore, generating non-classical correlations requires non-linear terms in the Hamiltonian. Depending on the type of atom-atom

interaction, one can differentiate between two schemes (see Fig. 3.1): Firstly, spin-dependent dynamics where a state dependent phase shift leads to a sheering on the Bloch sphere and thus redistributes the uncertainties. And secondly, spin-changing dynamics change the spin of single particles under conservation of the total spin.

3.1 Spin-dependent dynamics

In the case of spin-dependent dynamics, atoms in the same state collide, generating entanglement and realizing a one-axis twisting scheme. The Hamiltonian is given by $H_{OAT} = \chi J_z^2$ [40], where χ is the interaction strength. The dynamics can be visualized as a rotation around J_z depending on J_z. The uncertainty distribution is thereby redistributed, leading to an effective shearing. This dynamics were first observed in ^{87}Rb Bose-Einstein condensates [27, 41] between the states in the level $|\mathcal{A}\rangle = |F = 1, m_F = -1\rangle$ and $|\mathcal{B}\rangle = |F = 2, m_F = +1\rangle$. To study this scheme the collisional interactions defined as $U_{i,j} = 2\pi a^{i,j}/m \int d^3r |\Psi_i(r)|^2 |\Psi_j(r)|^2$ with the s-wave scattering length $a^{i,j}$ and the atomic mass m have to be considered. The inter-species collisional interaction $U_{\mathcal{A},\mathcal{B}}$ has to be reduced with respect to the intra-species interactions $U_{\mathcal{A},\mathcal{A}}$ and $U_{\mathcal{B},\mathcal{B}}$ to increase the interaction strength $\chi = U_{\mathcal{A},\mathcal{A}} + U_{\mathcal{B},\mathcal{B}} - 2U_{\mathcal{A},\mathcal{B}}$ [15]. The interaction strength is typically nearly zero, because $U_{\mathcal{A},\mathcal{A}} + U_{\mathcal{B},\mathcal{B}} \approx 2U_{\mathcal{A},\mathcal{B}}$. Increasing the interaction strength or equivalently reducing the term $U_{\mathcal{A},\mathcal{B}}$ has so far been realized in two different ways, either with a state selective microwave potential [27] or by utilizing a Feshbach resonance [41] (see Fig. 3.1). This dynamics was be performed on an atom chip and in an optical dipole trap, respectively. One-axis twisting dynamics creates spin-squeezed states at short evolution times. A value of $8.2\,\mathrm{dB}$ spin squeezing beyond the standard quantum limit was reached with detection noise subtracted in Ref. [41]. For longer evolution times, over-squeezed states are created, which are still useful for metrology beyond the the standard quantum limit. However, their evaluation is much more complicated. Experimentally, they can be detected by measuring the Fisher information [29]. At an even longer squeezing time of $\chi t = \pi/2$, one-axis twisting generates a $NOON$ state $|\Psi_{NOON}\rangle = 1/\sqrt{2}(|N\rangle_{\mathcal{A}} |0\rangle_{\mathcal{B}} + \mathrm{e}^{iN} |0\rangle_{\mathcal{A}} |N\rangle_{\mathcal{B}})$ allowing for Heisenberg limited metrology [15]. These states are extremely sensitive, i.e. they are destroyed if a single spin is measured. Because of this extreme sensitivity, $NOON$ states have so far not been experimentally realized in Bose-Einstein condensates.

3.2 Spin-changing dynamics: Hamiltonian

The second scheme is an analog to optical parametric down conversion and is sketched in Fig. 3.2. It utilizes the phase transitions in ^{87}Rb Bose-Einstein condensates to create non-classical states. The $F = 1$ manifold is in general used for experiments [42, 43, 44, A1, A2, A3, A4]. The many-body Hamiltonian can be written as $H_{\mathrm{SD}} = (q + E_n)(N_{+1} + N_{-1}) + 2CU_1(a_0^\dagger a_0^\dagger a_{+1} a_{-1} + a_0 a_0 a_{+1}^\dagger a_{-1}^\dagger)$ with $N_i = a_i^\dagger a_i$ with $i = +1, 0, -1$. The energy difference
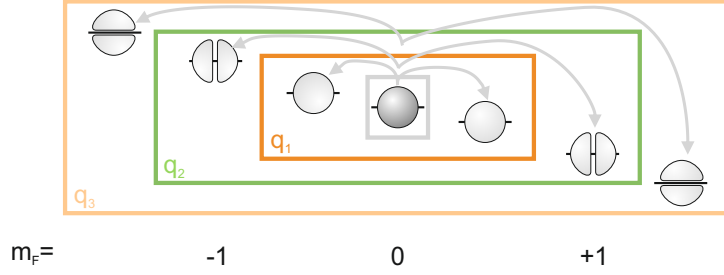
Figure 3.2: Sketch of spin-chaning collisions for three different values of q. Each value is resonant to a different mode. The mode structures are indicated as gray shaded areas.

$2q$ of two atoms in $|0\rangle$ compared to an atom pair in $|\pm 1\rangle$ can be identified as quadratic Zeeman energy. N_l with $l = -1, 0 + 1$ stands for the atom number in the respective Zeeman level. E_n denotes the eigenenergies of the effective potential $V = V_{\text{ext}} + (U_0 + U_1)n_0(\mathbf{r}) - \mu$ with the external trapping potential V_{ext}, the mean field term $(U_0 + U_1)n_0(\mathbf{r})$ and chemical potential μ. The last term $2CU_1(a_0^\dagger a_0^\dagger a_{+1}a_{-1} + a_0 a_0 a_{+1}^\dagger a_{-1}^\dagger)$ represents the spin-changing dynamics of the system. The overlap integral C is given by $\int \phi_{+1}^*(\mathbf{r})\phi_{-1}^*(\mathbf{r})\phi_0(\mathbf{r})\phi_0(\mathbf{r})d\mathbf{r}$ between the corresponding modes of the Zeeman levels. The interaction parameter U_1 describes the collisions of two atoms in $|0\rangle$ and changing their spins to $|\pm 1\rangle$ and is given by $U_1 = 4\pi(l_2 - l_0)/3m$ with the scattering lengths l_2 and l_0 and the atomic mass m. The ground state in the polar phase is given in the Fock basis by $|N_{+1}, N_0, N_{-1}\rangle = |0, N, 0\rangle$. At high values of q, in the twin Fock phase, the energy is minimized for the state $|N/2, 0, N/2\rangle$. Between these phases lies the broken-axisymmetry phase in which the ground state is described by the superposition $\sum_{k=0}^{N/2} d_k |k, N_0 - 2k, k\rangle$.

In the low depletion limit $N_0 \approx N = N_{+1} + N_0 + N_{-1} \gg 1$, the parametric approximation can be applied $a_0 \to \sqrt{N}$, which transforms the Bloch sphere into a plane (see Fig. 2.1b). On resonance $q = -E_n$ and at short times the Hamiltonian Bose-Einstein condensateomes $H_{\text{SD}} \approx \Omega(a_{+1}^\dagger a_{-1}^\dagger + a_{+1}a_{-1})$ with $\Omega = 2CU_1N_0$ generating the two-mode squeezed vacuum. By applying the basis change from $|+1\rangle$ and $|-1\rangle$ to $|S\rangle$ and $|A\rangle$, the Hamiltonian transforms into $H_{\text{SD}} = \Omega/2[(a_S^\dagger a_S^\dagger + a_S a_S) - (a_A^\dagger a_A^\dagger + a_A a_A)]$. The two-mode squeezed state is in the base of $|S\rangle$ and $|A\rangle$ transfromed into two single-mode squeezed states. The squeezing can then be visualized on two Bloch spheres with the modes $|S\rangle, |0\rangle$ and $|A\rangle, |0\rangle$. The change in q can be performed in different ways (see Fig. 3.1), which are discussed in the next paragraph.

Spin-changing dynamics: Quench, Ramp and Modulation of q

By quenching q the system cannot follow adiabatically, which results in a population of excited eigenstates of H_{SD}. For short evolution times, a two-mode squeezed state is created, which has been detected in Refs. [45, 32, A1, A2]. Up to $8.3\,\text{dB}$ squeezing beyond the standard quantum limit have been demonstrated so far [32]. For longer times, a large fraction of the Bose-Einstein condensate is transferred. The point of view also changes, the correlation manifest between the modes in the levels $|\pm 1\rangle$. The resulting twin Fock state exhibits multi-particle entanglement [46] and is useful for quantum metrology beyond the

shot-noise limit [43].

Instead of quenching, q can be ramped almost adiabatically as proposed in Ref. [47]. This technique was demonstrated in Refs. [23, 33, 34]. The speed of a system to follow a ramp adiabatically depends on the size of the energy gap between the ground and first excited state. The gap size at the phase transition scales with $N^{-1/3}$. This behavior was studied in Ref. [34]. Owing to atom losses in the $35\,\mathrm{s}$ ramp from the polar into the broken-axisymmetry phase no entanglement is detected. A number squeezing of $10.7\,\mathrm{dB}$ is reached by ramping into the twin Fock phase [23]. After the $3\,\mathrm{s}$ ramp a minimum of 910 atoms are entangled. The non-adiabaticity of this ramp results in oscillations in the broken-axisymmetry phase. However, this has not strongly influenced the conversion efficiency of $96\,\%$, taking the atom loss of $10\,\%$ not into account.

Another possibility is to modulate q periodically in time. If the modulation frequency is around $2q$, atom pairs from $|0\rangle$ can be excited into the states $|\pm1\rangle$. To modulate the quadratic Zeeman term in time, one can either change the magnetic field [35] or use a near-resonant microwave field oscillating in intensity [A3]. The resonances depend on different parameters. While the modulation amplitude has no influence on the resonance position, mean-field interactions have [35 ,A3]. In our work [A3], this effect manifests strongly on mode position of the excited states of the trapping potential.

Dynamical Casimir Effect

If the modes of the excitation are empty before initiating the dynamics, the excitation is a pure quantum mechanical effect, because a classical oscillator cannot be parametrically amplified from the ground state. This effect is analogous to the dynamical Casimir effect [48, 49] as described in Ref. [A3]. Ref. [35] used the same setup and showed $5\,\mathrm{dB}$ squeezing. However, this could be a result of a loss of contrast and does therefore not proof entanglement. The verification of entanglement and with this the verification of the underlying pair creation process is added in Ref. [A3]. Continuous-variable entanglement is demonstrated with a significance of 2.9 standard deviations [A3].

Other approaches use momentum states to measure analogues to the dynamical Casimir effect with cold atoms. In Ref. [50], superfluid Cesium is quenched with a jump in the magnetic field near a Feshbach resonance. The ensemble is initiated in its vibrational ground state. The quench gives rise to excitations manifesting as density fluctuations of the cloud. The interference of these excitations is studied, which leads to emergence of different momenta in dependence of the time after the quench. This phenomenon is also an analogue to Sakharov oscillations [51]. In Ref. [52], the speed of sound in a Bose-Einstein condensate is modulated with the external trapping potential generating Bogoliubov excitations. These excitations are detected with a position- and time-sensitive detector and the correlations between the different velocity classes are studied. While a quench of the trap frequency leads to a broad velocity distribution, a modulation results in a well-defined velocity class. However, no quantum correlations could be measured using second-order correlations functions. One possible explanation for this fact is that thermal and not vacuum fluctuations lead to the excitations.

All three ways to change q create non-classical states, while the needed time and resulting state depend on the used type.

3.3 Methods utilizing the external degrees of freedom

One possibility to create correlations between the atoms of a Bose-Einstein condensate utilizes different trap modes. Therefore, the position of an elongated optical dipole trap is changed rapidly in time to created excitations in a higher-order trap mode. The deexcitation into the ground mode is studied in Ref. [36]. To conserve energy and momentum, atom pairs with opposite momenta are created in an orthogonal direction. A Ramsey interferometer is realized between the ground and first excited state of the trap in Ref. [53]. Neither for the correlated momenta [36], nor for the two trap modes [53] sub-shot-noise fluctuations could be observed. In another approach a magnetic double-well potential is created with a radio-frequency field [37]. A full Mach-Zender interferometer between the atoms in the two wells is realized in Ref. [54]. Despite number squeezing of $5.7\,\mathrm{dB}$ is detected after the first beam splitter no sub-shot-noise phase resolution is achieved.

Another method applies an optical dipole trap superimposed with a moving optical lattice [38, 55]. The lattice creates correlated momentum pairs in a Bragg scattering process analogue to a four-wave mixing process. Mirrors and beam splitters can be realized with Bragg scattering. The different momentum classes are detected with a microchannel plate detector. In Ref. [38], this approach generates two modes with opposite momenta to measure an atomic analogue of the Hong-Ou-Mandel effect [56]. A second order correlation function is applied to analyze the momentum pairs. The scheme is extended in Ref. [55] to four modes. Due to the Bragg scattering, many momentum classes are generated. This opens the possibility to measure Bell correlations. Up to now, entanglement has not been proved yet[55].

Furthermore, an optical lattice can be used to split the Bose-Einstein condensate into different wells. In Ref. [39], this approach is used to split the condensate in up to six parts. Owing to tunneling of the atoms number squeezing can be detected between the wells. Additionally, a phase coherence factor is extracted out of the entanglement pattern, which in comparison with the number squeezing indicates entanglement.

4 Types of entangled states in Bose-Einstein condensates

Different classes of entangled states exist different properties. Unfortunately, there is no general scheme, that tests an entangled system to which class it belongs. Therefore, the different classes of entanglement need different indicators, that are especially designed for them. An overview of relevant different classes of entangled states and how to prove them is given in this chapter (see Fig. 4.1).
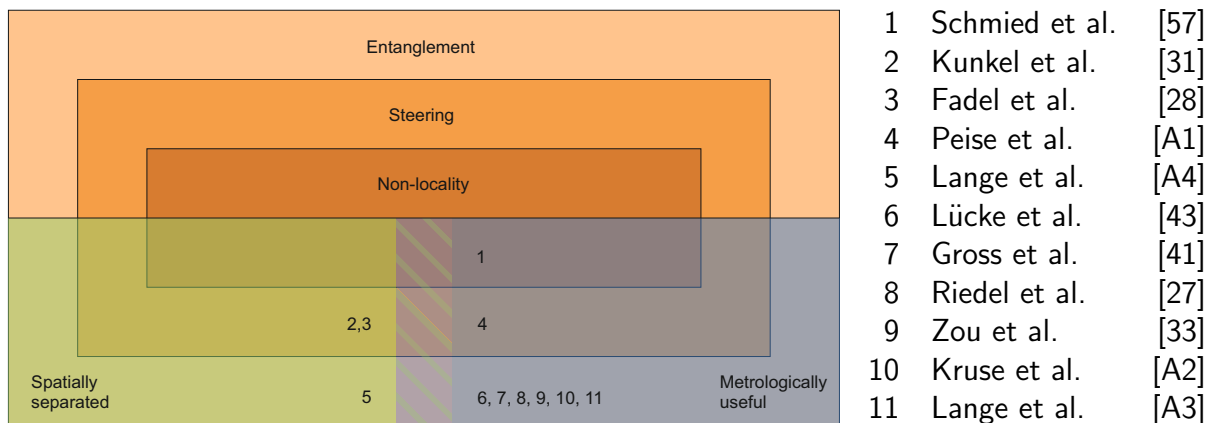
1	Schmied et al. [57]
2	Kunkel et al. [31]
3	Fadel et al. [28]
4	Peise et al. [A1]
5	Lange et al. [A4]
6	Lücke et al. [43]
7	Gross et al. [41]
8	Riedel et al. [27]
9	Zou et al. [33]
10	Kruse et al. [A2]
11	Lange et al. [A3]

Figure 4.1: Overview of relevant classes of entangled states and experimental demonstrations with Bose-Einstein condensates. A strict subclass to entangled states are the Einstein-Podolsky-Rosen correlated states, which violate an inferred Heisenberg uncertainty relation and therefore allow for steering. States, which violate a Bell inequality, are a strict subclass of Einstein-Podolsky-Rosen correlated states. These states can be used to show non-locality. All entangled states can be further divided into metrologically useful and spatially separated states.

4.1 The thought experiment of Einstein, Podolsky and Rosen

Einstein, Podolsky and Rosen (EPR) questioned the completeness of quantum mechanics in their famous paper from 1935 [58]. They assume a perfectly correlated system: A source emits two particles $\mathcal{A}$ and $\mathcal{B}$ with opposite momenta at the same time (see Fig. 4.2). Therefore, the positions of both particles with respect to the source are perfectly correlated, while their momenta are perfectly anti-correlated. By measuring the position (or momentum) of particle $\mathcal{A}$, the position (or momentum) of particle $\mathcal{B}$ can be precisely predicted. If both observables are measured in different realizations, it predetermines the outcome of a measurement. This is forbidden in quantum mechanics, because their uncertainties are subject to the Heisenberg uncertainty $\Delta P_{\mathcal{B}} \Delta X_{\mathcal{B}} \geq 1/2$. Thus the authors conclude that quantum

mechanics has to be incomplete. In Schrödinger's response [59, 60], this seeming violation of Heisenberg uncertainty principle was described by introducing the term entanglement and he brought up the idea that a measurement on one subsystem steers the outcome of the other subsystem. Nowadays, every non-separable state is called entangled. A clear definition and how entanglement can be measured is given in the next section.

4.2 Separability criteria

A pure product state of a bipartite system with the respective density matrices ρ^l with $l = \mathcal{A}, \mathcal{B}$ can be written as $\rho^\mathcal{A} \otimes \rho^\mathcal{B}$. A mixed product state can be seen as a sum of pure states weighted by the probability p_i for the ith state. Every state that cannot be written in the form $\rho = \sum_i p_i \rho_i^\mathcal{A} \otimes \rho_i^\mathcal{B}$ is bipartite entangled [61]. For a more general scenario, it follows that every separable state can be written as linear combination of pure state density matrixes [62]. The question if a given density matrix is entangled or not is called the separability problem. No general solution to this problem exists up to now.

It is practically favorable to differentiate between discrete- and continuous-variable entanglement. The Peres-Horodecki criterion is sufficient for the 2×2 and 2×3 dimensional case for discrete variables [63]. A general overview about discrete-variable separability criteria is given in Ref. [61]. The Peres-Horodecki criterion can be transferred to continuous variable systems [64]. This criterion is equivalent with Ref. [65] relying only on second-order moments. Therefore, this criterion is well suited to verify entanglement of quadrature squeezed states. The quadratures along two orthogonal directions have to be measured and the fluctuations of their sum or respectively their difference has to stay below two times the standard quantum limit $V_X^- + V_P^+ < 2$. In Ref. [A1], we measured this sum to be $V_X^- + V_P^+ = 0.85$ and violated the criterion with 15 standard deviations, while in Ref. [A3] the criterion was violated with 2.3 standard deviations. This shows non-separability of the identical atoms in our Bose-Einstein condensate. However, how is entanglement be defined between indistinguishable particles?

4.3 Identical particles and entanglement

Bose-Einstein condensates with seemingly thousands of entangled particles have been created [23]. The origin of many-particle entangled states in Bose-Einstein condensates lies in the symmetrization principle. For Bosons, every state has to be symmetrized over all particles per definition, which leads to this high degrees of entanglement. On the other hand, for entangled states it must be possible to define distinguishable subsystems. Furthermore, these subsystems must be able to exist as separate systems [66]. These requirements are necessary to the original concept of entanglement to make sense and rule out individual particles. In this sense, entanglement in Bose-Einstein condensate's can be seen as a mathematical artifact due to the symmetrization of the state [67, 68]. The next three sections show the usefulness of entangled Bose-Einstein condensate's. The last section shows how this opposition can be solved.

4.4 Metrologically useful entanglement

Every classical interferometer is limited by standard quantum limit. There are different ways to overcome this bound. One possibility is to use classical input states in combination with a non-linear beam splitter, which generates entanglement. This scheme is realized in Ref. [41] reaching $2.1\,\mathrm{dB}$. Increasing the atom number is strongly intertwined with the squeezing generation. To decouple these processes, the empty vacuum port can be squeezed, realizing Caves's squeezing [69]. We demonstrate this technique in Ref. [A2]. Firstly, spin-changing collisions create a quadrature-squeezed state. As described in the previous chapter, this process creates two single-mode squeezed states. The two input modes of the interferometer $|S\rangle$ and $|0\rangle$ are coupled with a radio-frequency pulse and the phase shift is realized by utilizing the clock transition $|1,0\rangle \to |2,0\rangle$. We realized $2.1\,\mathrm{dB}$ squeezing beyond the standard quantum limit with this scheme. Instead of squeezed states, other types of states can be utilized to generate sub-shot-noise resolution. For example, twin Fock states are applied to show an interferometric sensitivity of $1.6\,\mathrm{dB}$ beyond the standard quantum limit [43]. The input state was created with the quenching technique. Alternatively, a ramp can be used to create the non-classical input state [33]. A phase measurement precision of $2.05\,\mathrm{dB}$ beyond the two-mode standard quantum limit is reached with this technique. Furthermore, all three modes in $|0\rangle$ and $|\pm1\rangle$ can determine the interferometric phase. A resolution of $2.4\,\mathrm{dB}$ beyond the three-mode standard quantum limit is observed. A different kind of interferometer, an active $SU(1,1)$ interferometer, is realized in Ref. [70, 71]. Spin-changing collisions take the role of non-linear beam splitters. The disadvantage of this technique lies in the low number of atoms taking part in the interferometric sequence, while a large number of atoms is needed to initialize the dynamics.

4.5 Two-mode entanglement in spin space and Einstein-Podolsky-Rosen entanglement
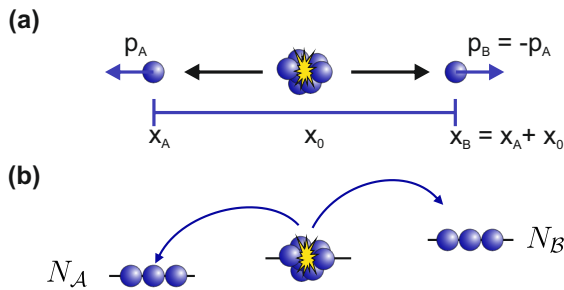

Figure 4.2: Einstein-Podolsky-Rosen entanglement: **(a)** in the original thought experiment and **(b)** between the spin states of ^{87}Rb.

The thought experiment of EPR, in which the result of one measurement on sub-system $\mathcal{A}$ can be used to predict the outcome sub-system $\mathcal{B}$ seemingly better than allowed by the Heisenberg uncertainty principle, defines an independent class of entanglement. The description of EPR entanglement is generalized for not perfectly correlated system. By measuring $X_\mathcal{A}$ and $P_\mathcal{A}$ it is possible to predict the outcome of a measurement on sub-system $\mathcal{B}$ with the uncertainties $\Delta X_\mathcal{B}^{\mathrm{inf}}$ and $\Delta P_\mathcal{B}^{\mathrm{inf}}$. These prediction uncertainties violate an inferred Heisenberg inequality $\Delta X_\mathcal{B}^{\mathrm{inf}} \Delta P_\mathcal{B}^{\mathrm{inf}} \geq 1/2$ for EPR entangled states. The directionality that measurements on sub-system $\mathcal{A}$ can be used to violate

such an inequality, is called steering. If one subsystem can steer another subsystem, the reversion is not necessarily true. A continuous-variable criterion $V_X^- \times V_P^+ < 1/4$ is developed to reveal EPR correlations for the symmetric case in which subsystem $\mathcal{A}$ can steer subsystem $\mathcal{B}$ and vice versa in Ref. [72]. The first measurement of EPR with massive particles is performed in Ref. [A1]. Spin-changing collisions are used to create a two-mode spin squeezed state (see Fig. 4.2). To access the quadratures and reveal EPR correlation between them atomic homodyne detection is applied. The product of the quadrature variances is measured, yielding $V_X^- \times V_P^+ = 0.18$ with 2.4 standard deviations below the threshold of $1/4$ of the EPR criterion. This violation reveals EPR correlations for the first time with massive particles in the spin degree of freedom and is also a proof of a two-way steering scenario. Furthermore, atomic homodyne detection is also demonstrated as a tool for quantum tomography to reconstruct the density matrix of the quantum state [A1].

4.6 Bell tests and correlations

The strongest form of entangled states are Bell correlated states. Bell pointed out that entanglement is incompatible with a local theory of nature [73]. He developed inequalities which can test for non-locality. Every entangled state which can be used to violate a Bell inequality is therefore called Bell correlated. The first loophole-free Bell test was performed in 2015 with electron spins [74]. The largest system violating a Bell inequality so far consist of 14 ions [75]. Performing Bell tests with Bose-Einstein condensates, which consist of a few hundred or thousand of atoms is of particular interest to study relations between global properties of the state and the underlying correlations which cause a violation of a Bell inequality. The challenge lies in the fact that typically only global measurements can be performed which do not allow to test the locally causal nature. Therefore, the term Bell test refers to tests of non-locality and measurements, which assume non-locality, prove Bell correlations. Witness inequalities rely on the assumption that the particles do not communicate or interact through unknown channels to relax the requirement that every observer can perform local measurements. Such a witness inequality is derived in Ref. [76] for a many-body quantum spin system. This witness was violated using a spin-squeezed Bose-Einstein condensate with a significance of 3.8 standard deviations below the threshold [57]. The same type of witness was violated with 124 standard deviations below the threshold by using cold atoms [77]. A Bell test with Bose-Einstein condensates has not been realized up to now.

4.7 Two-mode entanglement in the spatial degree of freedom

As shown in the previous sections spinor Bose-Einstein condensate's have been used to show EPR [A1] and Bell correlations [57]. However, the treatment of the indistinguishably of the atoms remains unsolved. There are several theoretical proposals how to make the atoms distinguishable without destroying the entanglement. One possiblity is to let the Bose-

Einstein condensate expand for a long time. The atomic cloud Bose-Einstein condensateomes so dilute that every particle can be individually addressed [78]. An alternative approach is given in Refs. [79, 80] where particle entanglement is converted into mode entanglement.
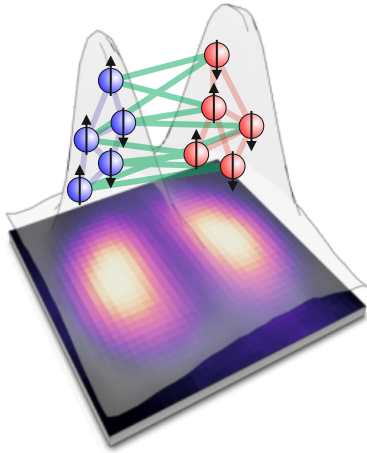

Figure 4.3: Entanglement between the two clouds (indicated by green lines) in the system is detected by analyzing spin correlations. The atomic density profile is shown in the background.

We realized this step in Ref. [A4]. By utilizing the mode structure of an excited trap mode (see Fig. 3.2) entanglement between two distinct atomic clouds has been measured. To perform the experiment up to 6000 atoms are transferred via spin-changing collisions (see Fig. 4.3). The resulting twin Fock state is split along a natural line of zero density. This step divides Bose-Einstein condensate into two distinguishable parts. This process also splits the twin Fock state in $|\pm1\rangle$ into two separated twin Fock states. To verify entanglement between the states a criterion especially sensitive for twin Fock states is developed and applied. A violation of 2.8 standard deviations is achieved, which shows that the entanglement and indistinguishability can be decoupled from each other. Complementary to our work, entanglement and EPR correlations are measured between different parts of a Bose-Einstein condensate. After generating the many-particle entangled state, the condensate expands either in free fall [28] or in a single-beam optical dipole trap [31]. Then, different patterns and splitting ratios of the atomic cloud are studied to confirm that the entanglement is distributed equally between all atoms [28]. While Refs. [28, A4] show only two-partite entanglement, Ref. [31] demonstrates up to five-partite entanglement. EPR correlations between different parts and splitting ratios of the atomic cloud are measured in Ref. [28]. One-way EPR steering could be observed up to a gap size between the parts of the Bose-Einstein condensate of around $4\,\mu$m. Two-way EPR steering between spatial regions is observed in Refs. [31, 28]. Furthermore, three-way steering and steering with a discarded fraction of $30\,\%$ of the Bose-Einstein condensate corresponding to a distance of $13\,\mu$m between the two parts is measured in Ref. [31]. These results show the flexibility of Bose-Einstein condensates, since entanglement is detected with different criteria and between different regions of the condensate. The fundamental aspect is resolved, that indistinguishability in a Bose-Einstein condensate can be revoked, while the entanglement is not destroyed. Furthermore, local properties of Bose-Einstein condensates can be used, for example in quantum information tasks or to perform a Bell test as shown in the outlook.

5 Outlook

Bell tests between spatially separated parts of Bose-Einstein condensates have not yet been performed, as shown in Fig. 4.1. The state created in Ref. [A4] can be utilized as a resource for such a test. The principle is sketched in the following.

In 1992, Yurke and Stoler proposed a Bell test with two independent single-particle sources [81]. The scheme transferred to our setup is sketched in Fig. 5.1a by setting the atom number of the two Fock states to one. A Bell inequality violation can be obtained even though the emitted particles are created with different sources, because the entanglement is created by the beam splitting process. The symmetrization principle leads to the entangled input state $1\sqrt{2}(|+1\rangle_\mathcal{A}|-1\rangle_\mathcal{B} + |-1\rangle_\mathcal{A}|+1\rangle_\mathcal{B})$. The entanglement is generated by the first beam splitting process with BS_{+1} and BS_{-1}, which entangles one Fock state with the vacuum. The second beam splitters BS_L and BS_R combine the output ports of the first beam splitters and by analyzing the correlations between the detected photons it is possible to violate a Bell inequality.
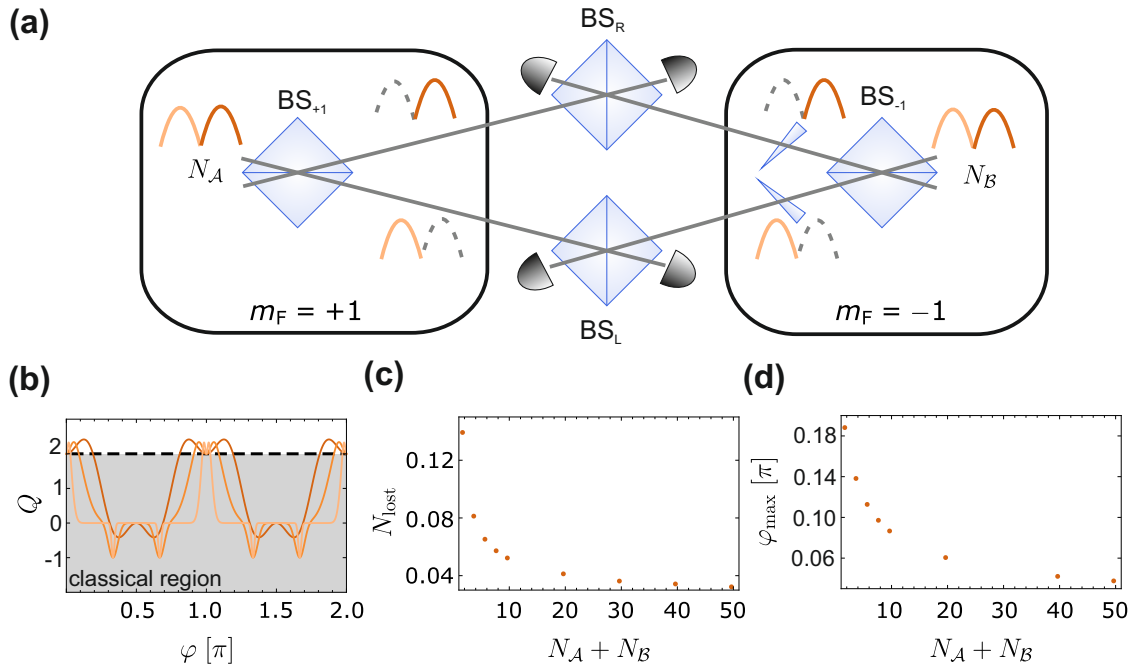

Figure 5.1: Bell test with two Fock states: **(a)** The idea of Ref. [82] adapted to our setup: The two Fock states are created with spin-changing collisions in the levels $m_\mathsf{F} = \pm 1$ in the first excited trap mode. **(b)** Bell violation witness Q for different phases. The colors stand for $N_\mathcal{A} + N_\mathcal{B} = 2$━, 10━, 100━. **(c)** Number of not detected atoms N_lost, which still lead to a Bell equality violation. **(d)** Angle resolution necessary to see a violation.

Laloë and Mullin extended this idea in two different ways for higher particle numbers [82] and for more participating Fock states [83]. The scheme for two Fock states can be adapted to our case. These states are created with spin-changing collisions in the levels $|\pm1\rangle$ in the first excited mode of the dipole trap. This ensures that both Fock states have the same

atom number $N_{\mathcal{A}} = N_{\mathcal{B}}$, for which the highest violation can be reached [82]. The setup is visualized in Fig. 5.1a. The spin-changing transfer into the first excited spatial mode of the trapping potential comprises the beam splitting process into a left and right well and hence realizing BS_{+1} and BS_{-1}.

The phase shift is only applied at the right part of the Bose-Einstein condensate. This shift can be realized with a detuned light field. To enable spatial addressability of the Bose-Einstein condensate, a beam dump can be used to block the light at the region of the left part. Therefore, the Bose-Einstein condensate has to be large enough. To ensure this, the phase shift pulse can be applied after a certain free fall time, in which the Bose-Einstein condensate expands. The beam splitters BS_R and BS_L can be realized by a microwave coupling between the states $|\pm 1\rangle$. In summary, all optical elements can be realized within our experiment. In a next step, the experimental requirements to observe a Bell inequality violation are discussed more quantitatively. Ref. [82] incorporates detection noise in the form of not-detected atoms. Since the Bell test relies on a parity measurement, this noise has to be smaller than one atom. Fig 5.1c shows the number of not-detected atoms as a function of the total number of particles, which can be accepted and still violate a Bell inequality. Because the absolute detection noise decreases with an increasing atom number it is favorable to perform the test with small atom numbers. Furthermore, as seen in Fig. 5.1b, the angle between the two parts has to be measured with high accuracy. The angle spread, at which a violation occurs, decreases with an increasing atom number, as shown in Fig. 5.1d. This in another reason to use Fock states with small atom numbers. In conclusion, this scheme can be adapted to Bose-Einstein condensates to perform a Bell test at our experiment.

6 Bibliography

[1] S. Gerlich, S. Eibenberger, M. Tomandl, S. Nimmrichter, K. Hornberger, P. J. Fagan, J. Tüxen, M. Mayor, M. Arndt. Quantum interference of large organic molecules. *Nat. Commun.* **2**, 263 (2011).

[2] K. Hornberger, S. Gerlich, P. Haslinger, S. Nimmrichter, M. Arndt. Colloquium: Quantum interference of clusters and molecules. *Rev. Mod. Phys.* **84**, 157 (2012).

[3] A. Bassi, K. Lochan, S. Satin, T. P. Singh, H. Ulbricht. Models of wave-function collapse, underlying theories, and experimental tests. *Rev. Mod. Phys.* **85**, 471 (2013).

[4] P. A. Altin, M. T. Johnsson, V. Negnevitsky, G. R. Dennis, R. P. Anderson, J. E. Debs, S. S. Szigeti, K. S. Hardman, S. Bennetts, G. D. McDonald, L. D. Turner, J. D. Close, N. P. Robins. Precision atomic gravimeter based on Bragg diffraction. *New Journal of Physics* **15**, 023009 (2013).

[5] Z.-K. Hu, B.-L. Sun, X.-C. Duan, M.-K. Zhou, L.-L. Chen, S. Zhan, Q.-Z. Zhang, J. Luo. Demonstration of an ultrahigh-sensitivity atom-interferometry absolute gravimeter. *Phys. Rev. A* **88**, 043610 (2013).

[6] T. L. Gustavson, P. Bouyer, M. A. Kasevich. Precision Rotation Measurements with an Atom Interferometer Gyroscope. *Phys. Rev. Lett.* **78**, 2046 (1997).

[7] J. K. Stockton, K. Takase, M. A. Kasevich. Absolute geodetic rotation measurement using atom interferometry. *Phys. Rev. Lett.* **107**, 133001 (2011).

[8] I. Dutta, D. Savoie, B. Fang, B. Venon, C. L. Garrido Alzar, R. Geiger, A. Landragin. Continuous Cold-Atom Inertial Sensor with $1 \ \mathrm{nrad/sec}$ Rotation Stability. *Phys. Rev. Lett.* **116**, 183003 (2016).

[9] N. Hinkley, J. A. Sherman, N. B. Phillips, M. Schioppo, N. D. Lemke, K. Beloy, M. Pizzocaro, C. W. Oates, A. D. Ludlow. An Atomic Clock with 10^{-18} Instability. *Science* **341**, 1215 (2013).

[10] N. Huntemann, C. Sanner, B. Lipphardt, C. Tamm, E. Peik. Single-Ion Atomic Clock with 3×10^{-18} Systematic Uncertainty. *Phys. Rev. Lett.* **116**, 063001 (2016).

[11] J. B. Fixler, G. T. Foster, J. M. McGuirk, M. A. Kasevich. Atom interferometer measurement of the newtonian constant of gravity. *Science* **315**, 74 (2007).

[12] G. Rosi, F. Sorrentino, L. Cacciapuoti, M. Prevedelli, G. M. Tino. Precision measurement of the Newtonian gravitational constant using cold atoms. *Nature* **510**, 518 (2014).

[13] P. Cladé, E. de Mirandes, M. Cadoret, S. Guellati-Khélifa, C. Schwob, F. Nez, L. Julien, F. Biraben. Precise measurement of h/m_{Rb} using Bloch oscillations in a vertical optical lattice: Determination of the fine-structure constant. *Phys. Rev. A* **74**, 052109 (2006).

17

[14] R. Bouchendira, P. Cladé, S. Guellati-Khélifa, F. Nez, F. Biraben. New Determination of the Fine Structure Constant and Test of the Quantum Electrodynamics. *Phys. Rev. Lett.* **106**, 080801 (2011).

[15] L. Pezzè, A. Smerzi, M. K. Oberthaler, R. Schmied, P. Treutlein. Quantum metrology with nonclassical states of atomic ensembles. *ArXiv e-prints* (2016).

[16] O. Hosten, N. J. Engelsen, R. Krishnakumar, M. A. Kasevich. Measurement noise 100 times lower than the quantum-projection limit using entangled atoms. *Nature* **529**, 505 (2016).

[17] S. L. Braunstein, P. van Loock. Quantum information with continuous variables. *Rev. Mod. Phys.* **77**, 513 (2005).

[18] N. Gisin, G. Ribordy, W. Tittel, H. Zbinden. Quantum cryptography. *Rev. Mod. Phys.* **74**, 145 (2002).

[19] S. Schreppler, N. Spethmann, N. Brahms, T. Botter, M. Barrios, D. M. Stamper-Kurn. Optically measuring force near the standard quantum limit. *Science* **344**, 1486 (2014).

[20] M. Nielsen, I. Chuang. Quantum Computation and Quantum Information. Cambridge University Press (2000).

[21] X.-L. Wang, L.-K. Chen, W. Li, H.-L. Huang, C. Liu, C. Chen, Y.-H. Luo, Z.-E. Su, D. Wu, Z.-D. Li, H. Lu, Y. Hu, X. Jiang, C.-Z. Peng, L. Li, N.-L. Liu, Y.-A. Chen, C.-Y. Lu, J.-W. Pan. Experimental Ten-Photon Entanglement. *Phys. Rev. Lett.* **117**, 210502 (2016).

[22] N. Friis, O. Marty, C. Maier, C. Hempel, M. Holzäpfel, P. Jurcevic, M. B. Plenio, M. Huber, C. Roos, R. Blatt, B. Lanyon. Observation of Entangled States of a Fully Controlled 20-Qubit System. *Phys. Rev. X* **8**, 021012 (2018).

[23] X.-Y. Luo, Y.-Q. Zou, L.-N. Wu, Q. Liu, M.-F. Han, M. K. Tey, L. You. Deterministic entanglement generation from driving through quantum phase transitions. *Science* **355**, 620 (2017).

[24] C. C. Gerry, P. Knight. Introductory quantum optics. Cambridge University Press (2005).

[25] A. I. Lvovsky. Squeezed light. In D. L. Andrews, editor, Photonics, Volume 1: Fundamentals of Photonics and Physics, chapter 5, 121–164. John Wiley & Sons (2015).

[26] A. I. Lvovsky, M. G. Raymer. Continuous-variable optical quantum-state tomography. *Rev. Mod. Phys.* **81**, 299 (2009).

[27] M. Riedel, P. Böhi, Y. Li, T. Hänsch, A. Sinatra, P. Treutlein. Atom-chip-based generation of entanglement for quantum metrology. *Nature* **464**, 1170 (2010).

[28] M. Fadel, T. Zibold, B. Décamps, P. Treutlein. Spatial entanglement patterns and Einstein-Podolsky-Rosen steering in Bose-Einstein condensates. *Science* **360**, 409 (2018).

[29] H. Strobel, W. Muessel, D. Linnemann, T. Zibold, D. B. Hume, L. Pezz, A. Smerzi, M. K. Oberthaler. Fisher information and entanglement of non-Gaussian spin states. *Science* **345**, 424 (2014).

[30] W. Muessel, H. Strobel, D. Linnemann, T. Zibold, B. Juliá-Díaz, M. K. Oberthaler. Twist-and-turn spin squeezing in Bose-Einstein condensates. *Phys. Rev. A* **92**, 023603 (2015).

[31] P. Kunkel, M. Prüfer, H. Strobel, D. Linnemann, A. Frölian, T. Gasenzer, M. Gärttner, M. K. Oberthaler. Spatially distributed multipartite entanglement enables EPR steering of atomic clouds. *Science* **360**, 413 (2018).

[32] C. D. Hamley, C. S. Gerving, T. M. Hoang, E. M. Bookjans, M. S. Chapman. Spin-nematic squeezed vacuum in a quantum gas. *Nature Phys.* **8**, 305 (2012).

[33] Y.-Q. Zou, L.-N. Wu, Q. Liu, X.-Y. Luo, S.-F. Guo, J.-H. Cao, M. Khoon Tey, L. You. Beating the classical precision limit with spin-1 Dicke state of more than 10000 atoms. *ArXiv e-prints* (2018).

[34] T. M. Hoang, H. M. Bharath, M. J. Boguslawski, M. Anquez, B. A. Robbins, M. S. Chapman. Adiabatic quenches and characterization of amplitude excitations in a continuous quantum phase transition. *Proc. Natl. Acad. Sci. U. S. A.* **113**, 9475 (2016).

[35] T. M. Hoang, M. Anquez, B. A. Robbins, X. Y. Yang, B. J. Land, C. D. Hamley, M. S. Chapman. Parametric excitation and squeezing in a many-body spinor condensate. *Nat. Commun.* **7**, 11233 (2016).

[36] R. Bücker, U. Hohenester, T. Berrada, S. van Frank, A. Perrin, S. Manz, T. Betz, J. Grond, T. Schumm, J. Schmiedmayer. Dynamics of parametric matter-wave amplification. *Phys. Rev. A* **86**, 013638 (2012).

[37] S. Hofferberth, I. Lesanovsky, B. Fischer, J. Verdu, J. Schmiedmayer. Radiofrequency-dressed-state potentials for neutral atoms. *Nature Physics* **2**, 710 (2006).

[38] R. Lopes, A. Imanaliev, A. Aspect, M. Cheneau, D. Boiron, C. I. Westbrook. Atomic Hong-Ou-Mandel experiment. *Nature* **520**, 66 (2015).

[39] J. Estève, C. Gross, A. Weller, S. Giovanazzi, M. K. Oberthaler. Squeezing and entanglement in a Bose-Einstein condensate. *Nature* **455**, 1216 (2008).

[40] M. Kitagawa, M. Ueda. Squeezed spin states. *Phys. Rev. A* **47**, 5138 (1993).

[41] C. Gross, T. Zibold, E. Nicklas, J. Estève, M. K. Oberthaler. Nonlinear atom interferometer surpasses classical precision limit. *Nature* **464**, 1165 (2010).

[42] M.-S. Chang, Q. Qin, W. Zhang, L. You, M. S. Chapman. Coherent spinor dynamics in a spin-1 Bose condensate. *Nature Phys.* **1**, 111 (2005).

[43] B. Lücke, M. Scherer, J. Kruse, L. Pezzé, F. Deuretzbacher, P. Hyllus, O. Topic, J. Peise, W. Ertmer, J. Arlt, L. Santos, A. Smerzi, C. Klempt. Twin Matter Waves for Interferometry Beyond the Classical Limit. *Science* **334**, 773 (2011).

[44] C. Klempt, O. Topic, G. Gebreyesus, M. Scherer, T. Henninger, P. Hyllus, W. Ertmer, L. Santos, J. J. Arlt. Parametric amplification of vacuum fluctuations in a spinor condensate. *Phys. Rev. Lett.* **104**, 195303 (2010).

[45] C. Gross, H. Strobel, E. Nicklas, T. Zibold, N. Bar-Gill, G. Kurizki, M. K. Oberthaler. Atomic homodyne detection of continuous-variable entangled twin-atom states. *Nature* **480**, 219 (2011).

[46] B. Lücke, J. Peise, G. Vitagliano, J. Arlt, L. Santos, G. Tóth, C. Klempt. Detecting multiparticle entanglement of Dicke States. *Phys. Rev. Lett.* **112**, 155304 (2014).

[47] Z. Zhang, L.-M. Duan. Generation of Massive Entanglement through an Adiabatic Quantum Phase Transition in a Spinor Condensate. *Phys. Rev. Lett.* **111**, 180401 (2013).

[48] E. Yablonovitch. Accelerating reference frame for electromagnetic waves in a rapidly growing plasma: Unruh-Davies-Fulling-DeWitt radiation and the nonadiabatic Casimir effect. *Phys. Rev. Lett.* **62**, 1742 (1989).

[49] J. Schwinger. Casimir energy for dielectrics: spherical geometry. *Proc. Natl. Acad. Sci. U. S. A.* **89**, 11118 (1992).

[50] C.-L. Hung, V. Gurarie, C. Chin. From Cosmology to Cold Atoms: Observation of Sakharov Oscillations in a Quenched Atomic Superfluid. *Science* **341**, 1213 (2013).

[51] A. D. Sakharov. The Initial Stage of an Expanding Universe and the Appearance of a Nonuniform Distribution of Matter. *JETP* **49**, 345 (1965).

[52] J.-C. Jaskula, G. B. Partridge, M. Bonneau, R. Lopes, J. Ruaudel, D. Boiron, C. I. Westbrook. Acoustic Analog to the Dynamical Casimir Effect in a Bose-Einstein Condensate. *Phys. Rev. Lett.* **109**, 220401 (2012).

[53] S. van Frank, A. Negretti, T. Berrada, R. Bücker, S. Montangero, J.-F. Schaff, T. Schumm, T. Calarco, J. Schmiedmayer. Interferometry with non-classical motional states of a Bose-Einstein condensate. *Nat. Commun.* **5**, 4009 (2014).

[54] T. Berrada, S. van Frank, R. Bücker, T. Schumm, J.-F. Schaff, J. Schmiedmayer. Integrated Mach-Zehnder interferometer for Bose-Einstein condensates. *Nat. Commun.* **4**, (2013).

[55] P. Dussarrat, M. Perrier, A. Imanaliev, R. Lopes, A. Aspect, M. Cheneau, D. Boiron, C. I. Westbrook. Two-Particle Four-Mode Interferometer for Atoms. *Phys. Rev. Lett.* **119**, 173202 (2017).

[56] C. K. Hong, Z. Y. Ou, L. Mandel. Measurement of subpicosecond time intervals between two photons by interference. *Phys. Rev. Lett.* **59**, 2044 (1987).

[57] R. Schmied, J.-D. Bancal, B. Allard, M. Fadel, V. Scarani, P. Treutlein, N. Sangouard. Bell correlations in a Bose-Einstein condensate. *Science* **352**, 441 (2016).

[58] A. Einstein, B. Podolsky, N. Rosen. Can quantum-mechanical description of physical reality be considered complete? *Phys. Rev.* **47**, 777 (1935).

[59] E. Schrödinger. Discussion of Probability Relations between Separated Systems. *Math. Proc. Cambridge Philos. Soc.* **31**, 555 (1935).

[60] E. Schrödinger. Probability relations between separated systems. *Proc. Cambridge Philos. Soc.* **31**, 555 (1935).

[61] O. Gühne, G. Tóth. Entanglement detection. *Phys. Rep.* **474**, 1 (2009).

[62] R. F. Werner. Quantum states with Einstein-Podolsky-Rosen correlations admitting a hidden-variable model. *Phys. Rev. A* **40**, 4277 (1989).

[63] A. Peres. Separability Criterion for Density Matrices. *Phys. Rev. Lett.* **77**, 1413 (1996).

[64] R. Simon. Peres-Horodecki Separability Criterion for Continuous Variable Systems. *Phys. Rev. Lett.* **84**, 2726 (2000).

[65] L.-M. Duan, G. Giedke, J. I. Cirac, P. Zoller. Inseparability Criterion for Continuous Variable Systems. *Phys. Rev. Lett.* **84**, 2722 (2000).

[66] B. J. Dalton, J. Goold, B. M. Garraway, M. D. Reid. Quantum entanglement for systems of identical bosons: I. General features. *Physica Scripta* **92**, 023004 (2017).

[67] G. Ghirardi, L. Marinatto. General criterion for the entanglement of two indistinguishable particles. *Phys. Rev. A* **70**, 012109 (2004).

[68] F. Benatti, R. Floreanini, U. Marzolino. Entanglement and squeezing with identical particles: ultracold atom quantum metrology. *J. Phys. B: At., Mol. Opt. Phys.* **44**, 091001 (2011).

[69] C. M. Caves. Quantum-mechanical noise in an interferometer. *Phys. Rev. D* **23**, 1693 (1981).

[70] D. Linnemann, H. Strobel, W. Muessel, J. Schulz, R. J. Lewis-Swan, K. V. Kheruntsyan, M. K. Oberthaler. Quantum-Enhanced Sensing Based on Time Reversal of Nonlinear Dynamics. *Phys. Rev. Lett.* **117**, 013001 (2016).

[71] D. Linnemann, J. Schulz, W. Muessel, P. Kunkel, M. Prüfer, A. Frölian, H. Strobel, M. K. Oberthaler. Active SU(1,1) atom interferometry. *Quantum Science and Technology* **2**, 044009 (2017).

[72] M. D. Reid. Demonstration of the Einstein-Podolsky-Rosen paradox using nondegenerate parametric amplification. *Phys. Rev. A* **40**, 913 (1989).

[73] J. S. Bell. On the Einstein-Podolsky-Rosen paradox. *Physics* **1**, 195 (1964).

[74] B. Hensen, H. Bernien, A. E. Dréau, A. Reiserer, N. Kalb, M. S. Blok, J. Ruitenberg, R. F. L. Vermeulen, R. N. Schouten, C. Abellán, W. Amaya, V. Pruneri, M. W. Mitchell, M. Markham, D. J. Twitchen, D. Elkouss, S. Wehner, T. H. Taminiau, R. Hanson. Loophole-free Bell inequality violation using electron spins separated by 1.3 kilometres. *Nature* **526**, 682 (2015).

[75] B. P. Lanyon, M. Zwerger, P. Jurcevic, C. Hempel, W. Dür, H. J. Briegel, R. Blatt, C. F. Roos. Experimental Violation of Multipartite Bell Inequalities with Trapped Ions. *Phys. Rev. Lett.* **112**, 100403 (2014).

[76] J. Tura, R. Augusiak, A. B. Sainz, T. Vértesi, M. Lewenstein, A. Acín. Detecting nonlocality in many-body quantum states. *Science* **344**, 1256 (2014).

[77] N. J. Engelsen, R. Krishnakumar, O. Hosten, M. A. Kasevich. Bell Correlations in Spin-Squeezed States of 500 000 Atoms. *Phys. Rev. Lett.* **118**, 140401 (2017).

[78] P. Hyllus, L. Pezzé, A. Smerzi, G. Tóth. Entanglement and extreme spin squeezing for a fluctuating number of indistinguishable particles. *Phys. Rev. A* **86**, 012337 (2012).

[79] N. Killoran, M. Cramer, M. B. Plenio. Extracting Entanglement from Identical Particles. *Phys. Rev. Lett.* **112**, 150501 (2014).

[80] M. S. Kim, W. Son, V. Bužek, P. L. Knight. Entanglement by a beam splitter: Nonclassicality as a prerequisite for entanglement. *Phys. Rev. A* **65**, 032323 (2002).

[81] B. Yurke, D. Stoler. Bell's-inequality experiments using independent-particle sources. *Phys. Rev. A* **46**, 2229 (1992).

[82] F. Laloë, W. J. Mullin. Interferometry with independent Bose-Einstein condensates: parity as an EPR/Bell quantum variable. *Eur. Phys. J. B* **70**, 377 (2009).

[83] W. J. Mullin, F. Laloë. Interferometer tests for quantum non-locality using Bose-Einstein condensates. *J. Phys. Conf. Ser.* **150**, 032068 (2009).

7 List of Publications and own contributions

[A1] J. Peise, I. Kruse, K. Lange, B. Lücke, L. Pezzè, J. Arlt, W. Ertmer, K. Hammerer, L. Santos, A. Smerzi and C. Klempt. Satisfying the Einstein-Podolsky-Rosen criterion with massive particles. *Nat. Commun.* **6**, 8984 (2015).

I helped performing the experiments and took part in the acquisition, analysis and interpretation of data and the revision of the manuscript.

[A2] I. Kruse, K. Lange, J. Peise, B. Lücke, L. Pezzè, J. Arlt, W. Ertmer, C. Lisdat, L. Santos, A. Smerzi and C. Klempt. Improvement of an atomic clock using squeezed vacuum. *Phys. Rev. Lett.* **117**, 143004 (2016).

I helped performing the experiments and took part in the acquisition, analysis and interpretation of data and the revision of the manuscript.

[A3] K. Lange, J. Peise, B. Lücke, T. Gruber, A. Sala, A. Polls ,W. Ertmer, B. Juliá-Díaz, L. Santos and C. Klempt. Creation of entangled atomic states by an analogue of the Dynamical Casimir Effect. *ArXiv e-prints*, arXiv:1805.02560 (2018).

I was involved in the conception of the work and had the main part in performing the experiments. I mostly acquired, analyzed and interpreted data and had a major part in writing manuscript.

[A4] K. Lange, J. Peise, B. Lücke, I. Kruse, G. Vitagliano, I. Apellaniz, M. Kleinmann, G. Tóth and C. Klempt. Entanglement between two spatially separated atomic modes. *Science* **360**, 416-418 (2018).

I had the main part in performing the experiments. I mostly acquired, analyzed and interpreted data and was involved in writing the manuscript.

8 Curriculum vitae

Persönliche Daten

Name	Karsten Lange
Geboren	am 16. Juli 1987 in Salzwedel

Bildungsweg

- Leibniz Universität Hannover
02/2015 - aktuell — Doktorarbeit am Institut für Quantenoptik

- Otto-von-Guericke Universität Magdeburg
01/2014 - 12/2014 — Diplomarbeit an der Fakultät für Naturwissenschaften in der Abteilung Materialphysik mit dem Titel *Einfluss der Elektronendichte auf die optische Anisotropie von hexagonalem Galliumnitrid*

- Otto-von-Guericke Universität Magdeburg
09/2009 - 12/2013 — Studium der Physik

- Gymnasium Beetzendorf
2000 - 06/2007 — Abitur

Berufserfahrung

- BHF-Bank Frankfurt
07/2009 - 09/2009 — Abteilung Strukturierte Außenhandelsfinanzierung

- BHF-Bank Frankfurt
2007 - 07/2009 — Ausbildung zum Bankkaufmann

9 Acknowledgments / Danksagung

Die Resultate dieser Arbeit konnten nur durch die liebevolle Unterstützung aller Beteiligten entstehen, denen ich an dieser Stelle danken möchte.

Allen voran spreche ich meinen herzlichen Dank meinem Doktorvater Carsten Klempt aus, der mir die Möglichkeit gab, mich in einem neuen Themenbereich der Physik beweisen zu können. Er war dabei stets für alle Belange ansprechbar, egal ob in der wöchentlichen Gruppenbesprechung oder beim täglichen Besuch im Café Kopi. Darüber hinaus stand er mir mit seiner Erfahrung und seinem fachkundigen Wissen stets zur Seite und hatte immer eine offene Tür. Auch die durch ihn initiierten täglichen gemeinsamen Mittagessen mit dem gesamten Team in der Mensa sorgten dafür, dass ich mich im Kollegium schnell wohl gefühlt habe. Weiterhin, möchte ich mich bei meinen Seniorkollegen Jan und Bernd bedanken, die mich mit offenen Armen aufgenommen haben. Jan hat mich während meiner gesamten Promotionszeit begleitet und war immer ein kompetenter und hilfsbereiter Ansprechpartner für alle Fragen. Besonders sein Wissen über die verschiedensten Bestandteile des Experiments und deren Funktionsweisen war oftmals eine nicht zu ersetzende Hilfe. Der Tag der Ersteinreichung von Ref. [A4] sei bespielhaft erwähnt. Als wir zusammen bis 23:55 Uhr letzte *kleine* Änderungen eingearbeitet haben, um die Veröffentlichung noch am selben Tag einzureichen. Dein Engagement und deine Kameradschaft waren vorbildlich für mich. Meinen jüngeren Kollegen Alexander und Fabian möchte ich ebenfalls danken. Ihr habt viele neue Impulse in die Arbeitsgruppe gebracht und ich weiß, dass *KRb* bei euch in guten Händen ist. Allen anderen Teammitgliedern unserer Arbeitsgruppe möchte ich gleichermaßen für die nette Zusammenarbeit danken.

Meinen Dank möchte ich an dieser Stelle auch Silke Ospelkaus für das Referieren meiner Arbeit und Wolfgang Ertmer für die Schaffung exzellenter Rahmenbedingungen für meine Promotion aussprechen. Weiterhin bedanke ich mich bei allen Mitgliedern der AG Rasel, dem Sekretariat und der Feinmechanikwerkstatt für ihre freundliche und hilfsbereite Art.

Géza Tóth möchte ich hier ebenfalls für das Referieren meiner Arbeit danken. Sein Theoriesupport war darüber hinaus unerlässlich für den Weg von der Idee zur Veröffentlichung von Ref. [A4].

Meinen Eltern, Birgit und Dieter, möchte ich für ihre Unterstützung danken. Ihr habt mir gezeigt, dass mir im Leben alle Wege offenstehen und ich mir meinen Weg aussuchen kann. Meinen Schwiegereltern, Dorothée und Stephan, möchte ich ebenfalls für ihr Interesse und ihre Unterstützung danken.

Mein größter Dank gilt meiner Frau, Inez. Am oben erwähnten Tag hast du uns noch von der Uni abgeholt und wir haben zusammen auf deinem gerade begonnenen Geburtstag angestoßen. Für alle Situationen hattest du immer Verständnis. Ohne die Kraft, die ich aus deiner Unterstützung bekommen habe, wäre diese Arbeit nicht möglich gewesen.